



# Evaluating contribution of *bis*-fluorination of selective $\gamma$ -lactam agonists towards rat EP<sub>4</sub> prostanoid receptor

Adam Uzieblo<sup>1\*</sup>, Melissa C Holt<sup>1\*</sup>, Rana Sidhu<sup>1</sup>, Chi S Ho<sup>1</sup>, Bradlee D Germain<sup>1</sup>, James B Kramer<sup>1</sup>, Andrei Kornilov<sup>1</sup>, Joseph M Colombo<sup>1</sup>, Fred L Ciske<sup>1</sup>,

Thomas A Owen<sup>2</sup>, Jeffrey K Johnson<sup>1</sup>, James P O'Malley<sup>2</sup>, María Inés Morano<sup>1</sup>, Stephen D Barrett<sup>1</sup>, Adam J Stein<sup>1</sup>

<sup>1</sup>Cayman Chemical, 1180 E. Ellsworth Rd., Ann Arbor, MI 48108; <sup>2</sup>Myometrics, LLC, 216 Howard Street, New London, CT 06320



## Introduction

### Abstract

The EP<sub>4</sub> prostanoid receptor is one of four G protein-coupled receptors (GPCRs) that mediate the actions of prostaglandin E<sub>2</sub> (PGE<sub>2</sub>; Item No. 14010). EP<sub>4</sub> is widely distributed in the body and plays various physiologic and pathophysiologic roles. In addition to classical inflammatory actions on immune cells, EP<sub>4</sub> is related to carcinogenesis, cardiac hypertrophy, vasodilation, vascular remodeling, bone remodeling, gastrointestinal homeostasis, renal function, and female reproductive function. Thus, the diverse EP<sub>4</sub>-mediated effects of PGE<sub>2</sub> point to the need to identify novel small molecule EP<sub>4</sub> agonists, both to further elucidate the function of this receptor subtype and for use in therapeutics. We have prepared a novel series of substituted gamma-lactam (pyrrolidinone) derivatives that mimic the carbocyclic prostaglandin scaffold structure and are potent, highly selective EP<sub>4</sub> agonists. Among them, two of Cayman's EP<sub>4</sub> agonists, KMN-80 (Item No. 15435) and KMN-159, only differ by difluoro substitution *alpha* to the lactam ring carbonyl group. In the present work these compounds were assessed against the *Rattus norvegicus* (rat) EP<sub>4</sub> homolog. EP<sub>4</sub> shares overlapping functional roles with other EP receptors. In particular, both EP<sub>4</sub> and EP<sub>2</sub> are coupled to G protein-dependent pathways through G<sub>αs</sub>, activating adenylate cyclase and inducing synthesis of intracellular cAMP. The biological function of the novel compound series was screened against the rat EP<sub>4</sub> receptor using Cayman's EP<sub>4</sub> Receptor (rat) Reporter Assay Kit (Item No. 600350), a luminescent cell-based cAMP response element reporter assay. Compounds were counterscreened for selectivity against Cayman's EP<sub>2</sub> Receptor (rat) Reporter Assay Kit (Item No. 600340). KMN-80 and KMN-159 are both potent EP<sub>4</sub> agonists with EC<sub>50</sub> values in the picomolar range and higher than 50,000-fold selectivity against EP<sub>2</sub>. Interestingly, *bis*-fluorination increased potency more than 5-fold within the SAR study. Compounds were evaluated further by docking onto the rat EP<sub>4</sub> and EP<sub>2</sub> receptor model using Schrödinger. The two fluoro groups in KMN-159 occupy hydrophobic space left unoccupied by the non-fluoro analog KMN-80, and the fluoro di-substitution flattens the lactam 5-membered ring, diminishing the strain on the sp<sup>2</sup> ring nitrogen while providing an entropic advantage. These stereoisomerically pure compounds represent a novel set of EP<sub>4</sub> receptor-selective agonists featuring a lactam core, a fully saturated heptanoic acid  $\alpha$ -chain, and a unique alkyne  $\omega$ -chain. *Bis*-fluorination *alpha* to the lactam ring carbonyl group further improves biological activation of the EP<sub>4</sub> receptor.

### Background

PGE<sub>2</sub> in humans is an almost ubiquitous arachidonic acid-COX cascade product that mainly mediates its multitude of signaling roles through activation of the GPCR superfamily-member E-type prostanoid receptors 1-4 (EP<sub>1-4</sub>). The roles of functionally related EP<sub>4</sub> and EP<sub>2</sub> receptors have been widely investigated, and the receptors have been considered as therapeutic targets for a variety of indications including cancer, asthma, inflammation, heart failure, colitis, ischemia, and osteoporosis. Selective EP<sub>4</sub> and EP<sub>2</sub> modulators have been sought to provide the benefits of target modulation while limiting side effects arising from the modulation of the other receptor subtypes. Both EP<sub>4</sub> and EP<sub>2</sub> are coupled to G protein-dependent pathways through G<sub>αs</sub> and, thus, activate adenylate cyclase and induce synthesis of intracellular cAMP.<sup>1</sup> Though EP<sub>4</sub> and EP<sub>2</sub> share overlapping functional roles, where they both are expressed in bone with roles in bone metabolism, they have only 38% homology in humans and are not pharmacologically identical.<sup>2</sup> It is reasonable to target highly EP<sub>4</sub> receptor-selective compounds as therapeutic agents.<sup>3,4</sup>

Roche reported a potent  $\gamma$ -lactam EP<sub>4</sub> receptor agonist, Compound 31, referred to here as CAY10684 (Cayman Item No. 15966).<sup>5</sup> This compound displayed essentially no binding affinity for EP<sub>2</sub>. The reported SAR suggested that replacing the PGE<sub>2</sub>  $\omega$ -chain pentyl terminus with an aromatic ring exploited some difference between the EP<sub>4</sub> and EP<sub>2</sub> binding sites, leading to the observed selectivity. Docking studies illustrate the fit and key binding interactions of CAY10684 within EP<sub>4</sub> and EP<sub>2</sub> binding site amino acid residues. Herein, we describe a Cayman SAR series focused on  $\omega$ -chain substitutions, utilizing an alkyne to provide rigidity. Additionally, the identification of the beneficial *bis*-fluorination of the  $\gamma$ -lactam greatly improved affinity. This work led to KMN-159, a novel, potent, and soluble EP<sub>4</sub>-selective agonist. Furthermore, we suggest its likely binding mechanism through docking studies which align well with the SAR series, focusing on the benefits of the *bis*-fluorination on the improved docking of KMN-159 over KMN-80 (Cayman Item No. 15435).

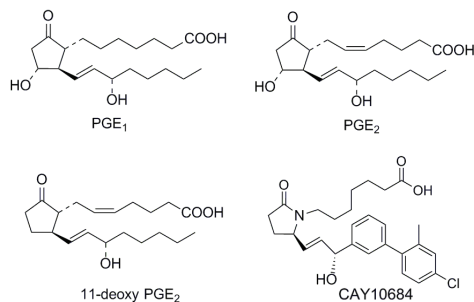


Figure 1 – Select EP<sub>4</sub> receptor agonists

## Methods

### Rat EP<sub>4</sub> Receptor Reporter Assay

A batch of frozen HEK293T cells were prepared and stored in vapor phase of a liquid nitrogen vessel. Aliquots of frozen HEK293T/17 cells were thawed and seeded onto a T150 tissue culture flask to allow recovery for 20-24 hours. Cells were harvested from the flasks and re-seeded on an EP<sub>4</sub> reporter assay plate (Cayman Item No. 600350) at a density of 65,000-75,000 cells/well in 200  $\mu$ l reduced serum medium containing 0.5% FBS. Cells were incubated at 37°C with 5% CO<sub>2</sub> for 16-18 hours to allow expression of the receptor target. Culture media was aspirated and replenished with 100  $\mu$ l serum-free culture medium. Test compounds were prepared at 2x final concentration and added to wells. For each compound, a 12-point dose-response curve (DRC) in 4-fold serial dilution was performed in triplicate. PGE<sub>2</sub> DRCs were run in parallel in all experiments (concentrations from 0-10 nM). After 6 hours of stimulation, 10  $\mu$ l of media was transferred to a corresponding well of a 96-well solid white plate. The plate was heated at 65°C for 30 minutes to inactivate endogenous alkaline phosphatase. Luminescence-based alkaline phosphatase substrate (Cayman Item No. 600183) was added to each well and Secreted Embryonic Alkaline Phosphatase (SEAP) activity was measured by reading the luminescence signal after a 10 minute incubation. The EC<sub>50</sub> values for PGE<sub>2</sub> and each test compound were calculated using GraphPad Prism 6 (GraphPad Prism version 6.00 for Windows, GraphPad Software, La Jolla California USA, www.graphpad.com). The methodology was performed with appropriate substitutions for assaying against rat EP<sub>2</sub> receptor.

### Rat EP<sub>4</sub> Receptor and Rat EP<sub>2</sub> Receptor Homology Modeling<sup>6</sup>

The sequences for *R. norvegicus* EP<sub>4</sub> receptor and *R. norvegicus* EP<sub>2</sub> receptor were submitted to RaptorX structure prediction suite (<http://raptorx.uchicago.edu/>) and analyzed to confirm the quality of the model using the P-value, global distance test, absolute global quality, and RMSD. All metrics indicated the models were acceptable. RaptorX utilized squid and human rhodopsin as the primary templates for rat EP<sub>4</sub> threading and squid rhodopsin and rat neurotensin receptor 1 as the primary templates for rat EP<sub>2</sub> threading. For rEP<sub>4</sub>, residues 1-16, 201-288, 352-488 were identified as potentially disordered. For rEP<sub>4</sub>, residues 1-17, 52-64, 227-257, 324-357 were identified as potentially disordered. For both models, these regions largely consist of loops. The receptors were prepared for docking in AutoDock with MGLTools 1.5.7.

### Induced Fit Docking with Schrödinger Maestro 11<sup>7-12</sup>

All files were prepared and generated within Maestro 11. Ligands were prepared with LigPrep from SMILES using OPLS3 force field modified using EPIK. Molecules were desalted and featured all possible tautomers. Receptors were modified using Maestro Protein Preparation Wizard selecting default values. Positions of hydrogen bonds and torsion angles were refined prior to initiation. A search grid of 8,000 Å<sup>3</sup> was centered on residue TYR188 for rEP<sub>4</sub> receptor docking. A search grid of 8,000 Å<sup>3</sup> was centered on residue SER121 for rEP<sub>2</sub> receptor docking. Glide docking was performed and subsequently refined with PRIME to introduce residue flexibility within 5 Å of the binding site. Compounds were evaluated based on docking score, Emodel score, and GlideScore.

## Results

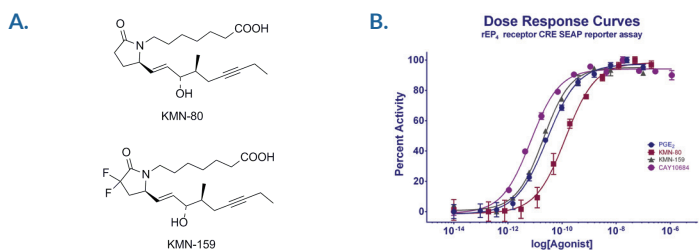


Figure 2 – A. Structures of KMN-80 and KMN-159. B. Representative data from rEP<sub>4</sub> receptor CRE SEAP reporter assay displaying dose-response curves for PGE<sub>2</sub>, KMN-80, KMN-159, and CAY10684.

Compound	EC <sub>50</sub> (μM) rEP <sub>4</sub> R	EC <sub>50</sub> (nM) rEP <sub>4</sub> R	RATIO EP <sub>2</sub> /EP <sub>4</sub>	rEP <sub>4</sub> R MAESTRO INDUCED FIT (kcal/mol)	rEP <sub>4</sub> R MAESTRO EMODEL	rEP <sub>4</sub> R MAESTRO INDUCED FIT (kcal/mol)	rEP <sub>4</sub> R MAESTRO EMODEL
PGE <sub>1</sub>	21.3±3.6 (n=3)	4.4±0.4 (n=3)	206	-10.72	-99.15	-11.08	-101.1
PGE <sub>2</sub>	29.2±1.5 (n=56)	3.3 (n=16)	113	-10.50	-99.2	-11.10	-113.72
11-DEOXY PGE <sub>2</sub>	36.9±10.7 (n=6)	38.71±4.48	1.049	-9.77	-87.83	-10.58	-83.83
CAY10684	6.9±0.06 (n=3)	>5,000	>724,637	-14.72	-149.97	-13.01	-116.56
KMN-159	26.5±2.7 (n=7)	4,900	184,905	-11.81	-111.93	-11.21	-94.74
KMN-80	166.61±14 (n=6)	>10,000	>60,000	-11.23	-103.06	-10.98	-94.47

Table 1 – Compiled data from rEP<sub>4</sub> receptor CRE SEAP reporter assay, rEP<sub>2</sub> receptor CRE SEAP reporter assay counter screen, AutoDock docking studies, and Schrödinger docking studies.

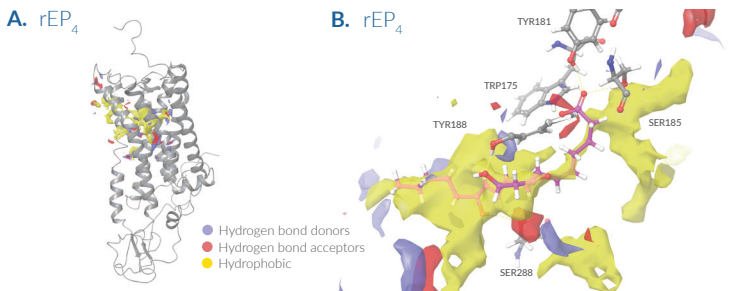


Figure 3 – A. RaptorX model of Rat EP<sub>4</sub> receptor with proposed ligand binding site identified and highlighted by Maestro 11 Ligand Site. B. Docking of PGE<sub>2</sub> into rEP<sub>4</sub> receptor model using a Maestro Induced Fit model, highlighting key interactions between the  $\alpha$ -chain carboxylate with TYR181 and TRP175, 15-hydroxyl with SER288, and 11-hydroxyl with TYR188. Side chains are displayed in gray.

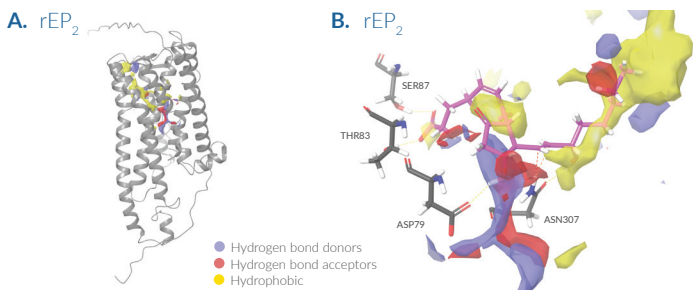


Figure 4 – A. RaptorX model of rat EP<sub>2</sub> receptor with proposed ligand binding site identified and highlighted by Maestro 11 Ligand Site. B. Docking of PGE<sub>2</sub> into rEP<sub>2</sub> receptor model using a Maestro Induced Fit model, highlighting key interactions between the 11-hydroxyl with ASP79,  $\alpha$ -chain carboxylate with SER87 and THR83, and 15-hydroxyl with ASN307. Side chains are displayed in gray.

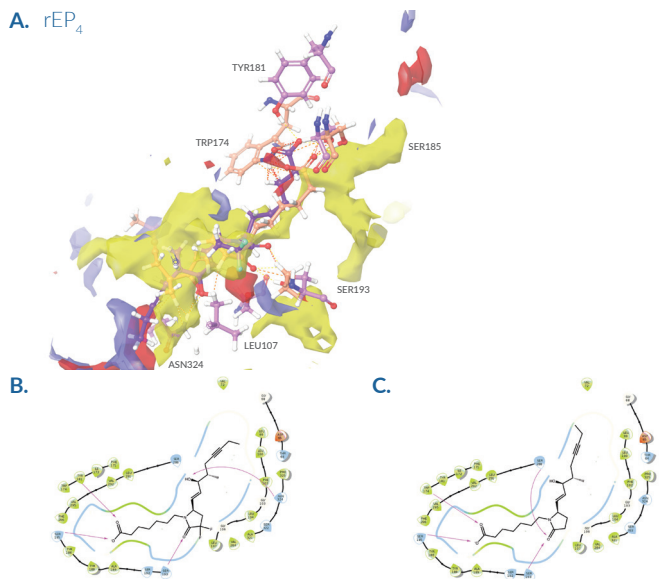


Figure 5 – A. Compound overlay of KMN-159, and KMN-80 to rEP<sub>4</sub> receptor generated from Maestro 11 Induced Fit model featuring site map. Side chains for each flexible dock are shown in either pale pink or pale orange. B. Key interactions for KMN-159 in 2D plot. C. Key interactions for KMN-80 in 2D plot.

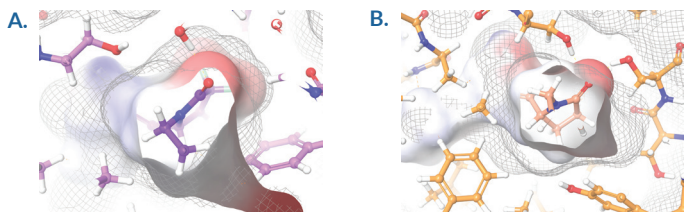


Figure 6 – A. Top docking pose of KMN-159 rEP<sub>4</sub> receptor generated from Maestro 11 Induced Fit model featuring surface representation of receptor and ligand binding site. B. Top docking pose of KMN-80 rEP<sub>4</sub> receptor generated from Maestro 11 Induced Fit model featuring surface representation of receptor and ligand binding site.

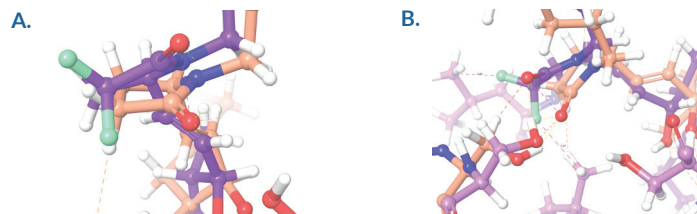


Figure 7 – A. Zoom in of puckered KMN-80 ring. B. Zoom in of flat KMN-159 ring.

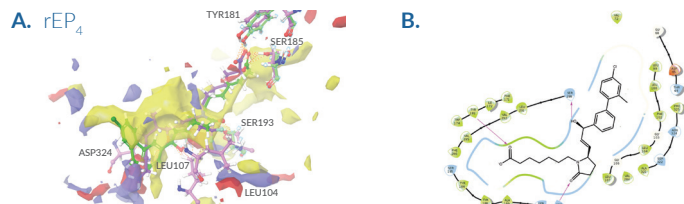


Figure 8 – A. Compound overlay of KMN-159 and CAY10684 featuring site map. Side chains for each flexible dock are shown in either pale pink or pale green. B. Key interactions of CAY10684 in 2D plot.



Figure 9 – A. Binding mode of PGE<sub>2</sub> with overlay of KMN-159 in rEP<sub>4</sub>, Maestro 11 Induced Fit model featuring site map. Note that KMN-159 does not sit in bottom of pocket like PGE<sub>2</sub>. Side chains forming PGE<sub>2</sub> binding pocket are ASP79, THR83, SER87, and ASN307 (gray). ASN307 makes a polar contact with KMN-159 carboxylate. B. Binding mode of PGE<sub>2</sub> with overlay of CAY10684 in rEP<sub>4</sub>, Maestro 11 Induced Fit model featuring site map. Note that CAY10684 does not overlap well and displays high internal torsion metrics.

## Conclusions

Key interactions were highlighted from this docking study regarding the binding of a series of novel rEP<sub>4</sub> receptor agonists. The lactam carbonyl is seen interacting with SER193 in nearly all compounds. A large hydrophobic pocket has been identified, which likely could be further exploited in the KMN series. SER185 is seen commonly locking the  $\alpha$ -chain carboxylate into place. Additionally, TYR181 and TRP174 are seen as interacting with the  $\alpha$ -chain carboxylate in some cases and not others. The 15-hydroxyl displayed the greatest variability and sensitivity in its interactions. In the case of KMN-80 versus KMN-159, we postulate that the increased size of the difluoro, coupled with the conformationally locked, flat nature of the 159  $\gamma$ -lactam, shifts the docked position of KMN-159 to create a more favorable hydrogen bonding interaction with the 15-hydroxyl relative to KMN-80 at a lower entropic cost. The increased potency of KMN-159 is a result of the interaction of the 15-hydroxyl with ASN324 and coordination of LEU104 and LEU107 by the difluoro moiety. These beneficial interactions are not present in KMN-80. KMN-159 displayed a very similar binding mode relative to CAY10684. CAY10684 displayed very strong metrics within the binding experiment. Additionally, compounds docked against the rEP<sub>2</sub> receptor displayed poorer metrics and did not overlay well with the natural substrates, particularly PGE<sub>2</sub>. These docking studies have allowed the interpretation of the SAR work in greater detail. The addition of the difluoro moiety is thought to play a small steric role, shifting the position of the lactam ring slightly, conformationally locking the  $\gamma$ -lactam, and improving the coordination of the carboxylate and 15-hydroxyl with their associated binding niches.

### References

1. Sugimoto, Y. and Narumisu, S. *J. Biol. Chem.* **282**(16), 11613-11617 (2007).
2. Blackwell, K.A., Raine, L.G., and Fribben, C.C. *Trends Endocrinol. Metab.* **20**(5), 294-301 (2010).
3. Ko, H.Z., Crawford, D.T., Qi, H., et al. *J. Bone Miner. Res.* **21**(4), 565-575 (2006).
4. Weinreb, M. and Shir, G.N. *Am. J. Physiol. Endocrinol. Metab.* **276**(2), E376-E383 (1999).
5. Elwerth, T.S., Kretzsch, D.J., Kim, W., et al. *Bioorg. Med. Chem. Lett.* **14**(7), 1655-1659 (2004).
6. Kilberg, M., Wang, H., Wang, S., et al. *Nat. Protoc.* **7**(8), 1511-1522 (2012).
7. Friesner, R.A., Murphy, R.B., Repasky, M.P., et al. *J. Med. Chem.* **49**(21), 6177-6196 (2006).
8. Halgren, T.A., Murphy, R.B., Friesner, R.A., et al. *J. Med. Chem.* **47**(7), 1739-1759 (2004).
9. Friesner, R.A., Banks, J.L., Murphy, R.B., et al. *J. Med. Chem.* **47**(7), 1739-1759 (2004).
10. Fard, R., Day, T., Friesner, R.A., et al. *Bioorg. Med. Chem.* **14**(9), 3160-3173 (2006).
11. Sherman, W., Day, T., Jacobson, M.P., et al. *J. Med. Chem.* **49**(2), 534-553 (2006).
12. Sherman, W., Beards, H.S., and Fard, R. *Chem. Biol. Drug Des.* **6**(7), 63-84 (2006).

\*These authors contributed equally to this work  
US Patent 9,180,116